Optical and Quantum Electronics **28** *(1996) 1669–1676*

Simulation of gain-switched picosecond pulse generation from quantum well lasers

H. A. TAFTI
School of Electronics and Communication Engineering, Anna University, Guindy, Madras-25, India

V. S. SHEEBA, K. K. KAMATH,* F. N. FAROKHROOZ, P. R. VAYA‡
Department of Electrical Engineering, Indian Institute of Technology, Madras-36, India

Received 16 June 1995; revised 23 March; accepted 22 April 1996

Circuit models for gain-switched quantum well laser diodes are developed and simulated using the circuit analysis program SPICE2. Effects of cavity length and number of wells on the output pulse shape are analysed. Picosecond pulses of 7 and 2 ps full-width at half-maximum (FWHM) are observed, corresponding to second and third quantized level transitions, respectively. A remarkable reduction in the output pulse width observed for the third quantized level transition, demonstrates the significance of higher sub-band transitions for ultrashort pulse generation.

1. Introduction

Picosecond pulse generation in multiple quantum well (QW) semiconductor lasers using the gain switching (GS) technique is gaining popularity, because enhanced differential gain in these lasers is effective for obtaining ultrashort pulses. So far, the gain switching characteristics of QW lasers have been investigated either experimentally or theoretically by the numerical solution of rate equations [1–4]. However, these methods suffer from the limitations of non-inclusion of substrate parasitics, package parasitics and device circuit interactions in the calculations. An alternate approach that overcomes these limitations is to transform the rate equations into a circuit model that can then be solved using standard circuit analysis techniques. In this paper, we have developed circuit models corresponding to multiple quantized state transitions (QST) for the generation of picosecond optical pulses in QW lasers. The model was simulated using the circuit simulation program SPICE2, and the effects of cavity length, L, and number of wells, N_w, on the output pulse shape, for various injection, I, current levels, were investigated.

2. Discussion

The optical gain function of single QW lasers shows a step-like behaviour in the transition

Present addresses: *Department of EECS, University of Michigan, USA. ‡Optoelectronics Laboratory, N U.S., Singapore.

0306–8919

TABLE I List of principal symbols and element values for the gain-switched model

Symbol	Definition	Value
c	Speed of light in vacuum	
c_g	Speed of light in the lasing medium	
C_D	Capacitance, diffusion (pf)	10.0000
C_p	Capacitance, photon (pf)	0.0672
C_{pp}	Capacitance, package parasitics (pf)	0.2300
E_0	Permittivity, free space	
f_c	Fermi distribution function, conduction band	
f_v	Fermi distribution function, valance band	
$g_{m1,2}$	Optical gain	
h	Planck's constant	
I	Injection current	
K	Boltzmann constant	
L_{pp}	Inductance, package parasitics (nh)	0.63
L_z	Active layer thickness (nm)	10
m_c^*	Effective mass, conductive band (m_e)	0.067
m_e	Electron mass	
m_r		
m_v^*	Effective mass, valence band (m_e)	0.450
n	Carrier density	
P	Photon density	
q	Electron charge	
R_{IN}	Resistance, pulse generator (Ω)	100.000
R_p	Resistance, photon (Ω)	21.182
R_{pp}	Resistance, package parasitics (Ω)	1.000
t		
T	Temperature (K)	300
V_a	Volume, active region	
W	Laser width (μm)	20
β	Spontaneous emission coefficient	2×10^{-4}
Γ	Optical confinement factor	0.03
$\mathcal{E}$	Gain compression factor (m^3)	4×10^{-23}
μ	Refractive index	3.55
τ_n	Carrier lifetime (ns)	3
τ_p	Photon lifetime	
ω	Radian frequency	

regime between $n = 1$ and $n = 2$ quantized state [5]. Therefore, the differential gain, dg/dn, that is responsible for the generation of short optical pulses, depends strongly on the operation conditions. The value of dg/dn can be higher by a factor of two for $n = 2$, in comparison to $n = 1$ sub-band transitions [6]. To model the gain switching process, including the effect of $n = 1$ and $n = 2$ quantized level interactions, we used a two-mode rate equation for the photon densities [3], given by:

$$\frac{dP_i}{dt} = \Gamma c_g g_{mi}(1 - \mathcal{E}P_i)P_i - \frac{P_i}{\tau_p} + \beta_i \frac{n}{\tau_n} \tag{1}$$

$$\frac{dn}{dt} = \frac{I}{qV_a} - c_g \sum g_{mi}(1 - \mathcal{E}P_i)P_i - \frac{n}{\tau_n} \tag{2}$$

where $i = 1, 2$, and the remaining terms are defined in Table I. Following the methodology described in [7], the above equations were transformed into the equivalent circuit shown in

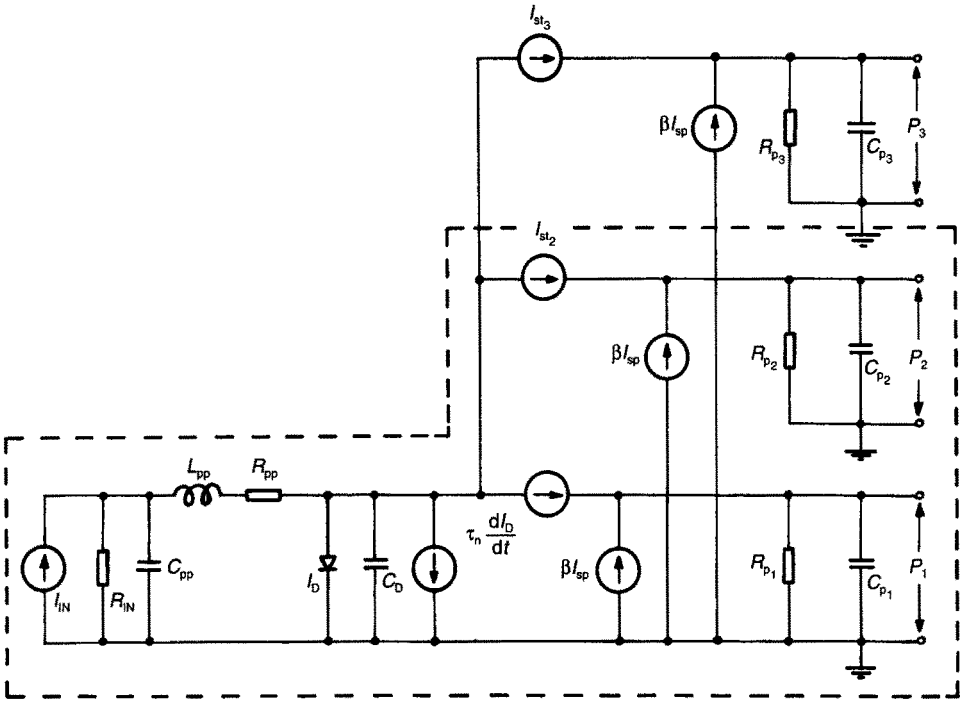

Figure 1 Circuit model representing the multiple quantized level in a QW laser diode. P_1, P_2 and P_3 are the output nodes for the $n = 1$, 2 and 3 levels, respectively.

Fig. 1 (enclosed within dashed lines): where the diode models the spontaneous recombination current; while the current generator, proportional to the time derivative of the spontaneous injection current, models the charge storage effects in the active layer. The diffusion capacitance is represented by C_D and the current component $I_{sp} = I_D$ represents the spontaneous emission. I_{stim} represents a polynomial current-controlled current source. Photon loss and storage are modelled by resistance, R_p, and capacitance, C_p, respectively. Figure 1, combined with package parasitics (where R_{IN} represents the resistance of the pulse generator; L_{pp}, the inductance; R_{pp}, small loss resistance; and C_{pp}, capacitance), is associated with the laser package [8, 9]. Each branch of the optical section corresponds to a quantized transition level in a QW laser. The spontaneous emission coefficient, β_i, is assumed to be a constant and the current generators, I_{st_1} and I_{st_2} are dependent on the gain. This gain is non-linear and is represented as a current source in the circuit model. Hence, the two branches of the optical section (for $i = 1$ and 2), that correspond to the $n = 1$ and 2 quantized state transitions, respectively, differ only in the differential gain coefficients. The model corresponds to a QW laser with an active layer thickness, L_z, of 10.0 nm, and it is validated by simulating the response to a direct current (d.c.) sweep as shown in Fig. 2. The input pulse amplitude is varied and simulations are performed. For a single QW laser (number of wells, $N_w = 1$) with cavity length $L = 160\,\mu$m, the result demonstrates that the laser emits only in the $n = 1$ quantized state at low injection levels (equivalently, $I < 0.5$ A), as shown in Fig. 3. Gain-switched picosecond pulses were observed when the input pulse amplitude was increased to $I = 0.5$ A (Fig. 4a). By reducing L to $140\,\mu$m, the critical amplitude of the input pulse required to achieve gain switching (Fig. 4b) is reduced to $I = 0.25$ A. Similar effects were observed in the case of a multiple QW laser. The dependency of the second level transition

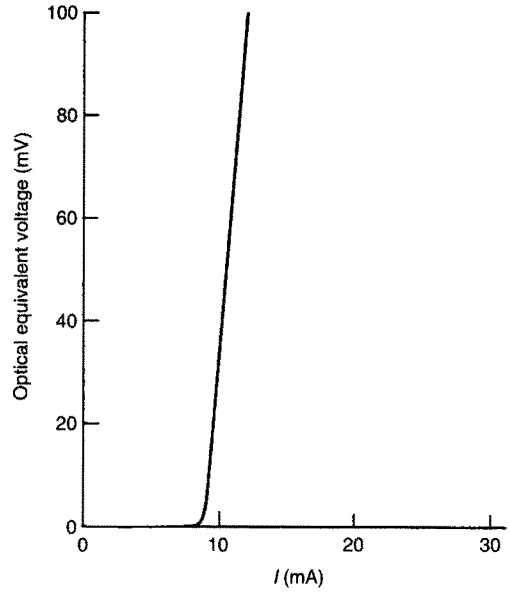

Figure 2 The d.c. L–I characteristics of a QW laser.

on the number of wells was determined by modifying the circuit model to represent a QW laser with two wells ($N_w = 2$). The results of the simulation are shown in Fig. 5. Gain-switched pulses were observed at $I = 1$ A and 0.5 A for $L = 80$ and 70 μm, respectively. Comparison of Figs 4 and 5 shows that gain switching is achieved at a lower value of input pulse amplitude in the case of a single QW laser. The above results, that indicate the importance of cavity length and number of wells, respectively, for observation of ultrashort pulses, are in excellent agreement with those obtained by other methods [1].

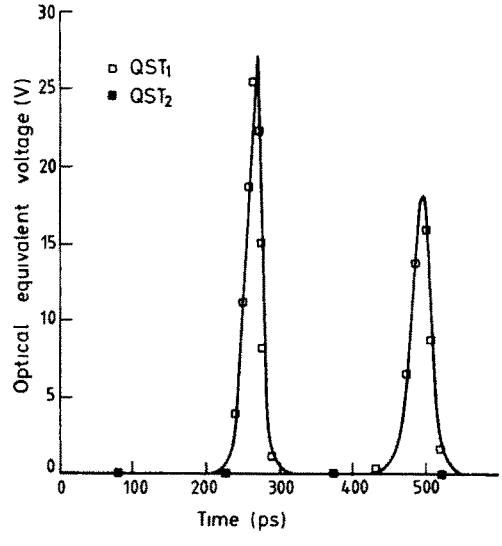

Figure 3 Simulated output pulse waveforms from a single QW laser with $L = 160$ μm: (□) QST1, (■) QST2.

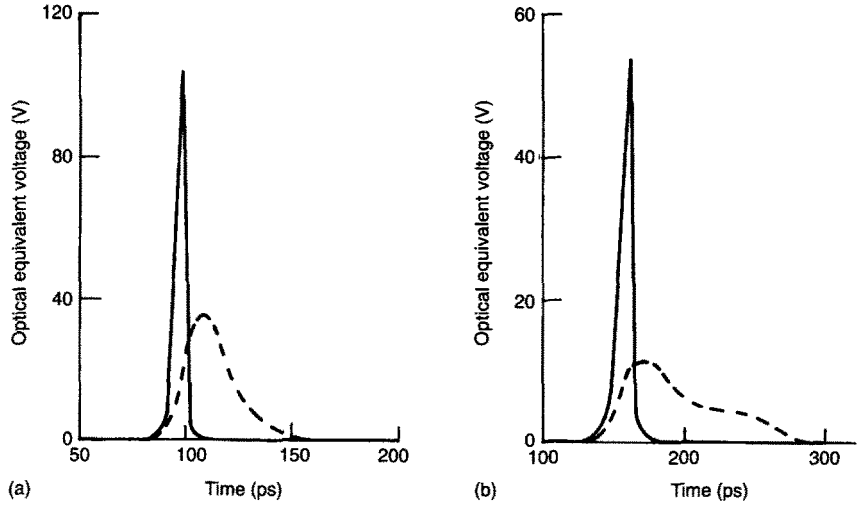

Figure 4 Output pulse waveforms from a gain-switched single QW laser with cavity length, L: (a) 160 μm and (b) 140 μm. (– – –) QST1, (——) QST2.

Further, the above model was simulated to study the effect of bias current on the output pulses. Figure 6 shows the total output corresponding to QST1 and QST2 for various bias currents. As the bias level increases, the pulse width decreases due to the increased domination of the QST2 transition, which gives an inherently sharper peak due to its higher differential gain.

It has been predicted that pulses generated due to higher-level transitions ($n > 2$) are particularly attractive for high-speed applications. Our calculations show that lasers with L_z below 10 nm lase at the second quantized state; whereas for L_z in excess of about 14.5 nm, the effect of the third quantized state transition (QST3) is observed. The gain–carrier density relationship for this level (for an AlGaAs laser with Al mole fraction $x = 0.25$) is shown in Fig. 7a. The

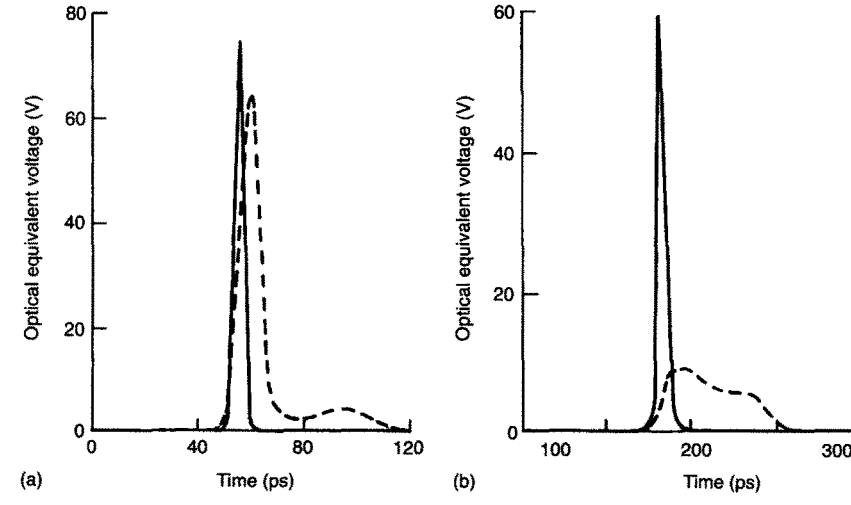

Figure 5 Simulated pulse waveform from a gain-switched multiple QW laser with $N_w = 2$. L: (a) 80 μm and (b) 70 μm. (– – –) QST1, (——) QST2.

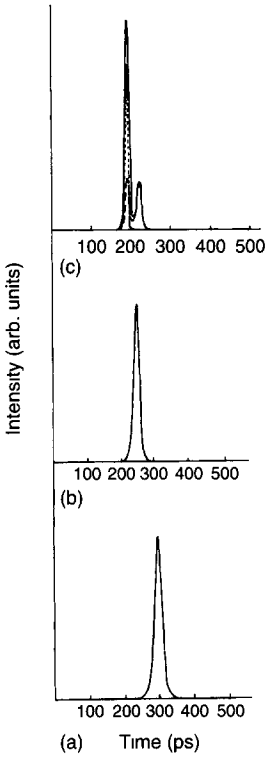

Figure 6 Simulated total optical output from a QW laser diode operating at two quantized levels, QST1 (– – –) and QST2 (- - - -), at I_{bias}: (a) 0.1, (b) 0.4, and (c) 0.8 I_{TH}.

gain–carrier density relationship is determined for the $n = 1$ transition by considering the gain expression [10–12]:

$$g_{m1} = K[f_c(E_{f_c}, E_{c_1}) - f_v(E_{f_v}, E_{v_1})] \tag{3}$$

where $K = 4\pi q^2 m_r / E_0 m_e^2 c\mu h L_z E_p$. $|M_b|^2$ is independent of carrier density and the quantity $|M_b|^2 = 1.3\, m_c E_q$ is the momentum matrix element of transition between the band edges. f_c (E_{f_c}, E_c) and f_v (E_{f_v}, E_v) are the Fermi distribution functions in conduction and valence bands, respectively; and E_c and E_v are given as:

$$E_c = \frac{m_r}{m_c^*}(E_p - E_g) \tag{4}$$

$$E_v = \frac{m_r}{m_v^*}(E_p - E_g) \tag{5}$$

$$m_r = \frac{m_c^* m_v^*}{(m_c^* + m_v^*)} \tag{6}$$

$$E_p = h\omega \tag{7}$$

Considering the lowest-order quantum transition, the electron density in the QW is obtained from [13]:

$$n = \frac{m_c^* KT}{\pi h^2 L_z} \ln\left[1 + \exp\left(\frac{E_{f_c} - E_{c_1}}{KT}\right)\right] \tag{8}$$

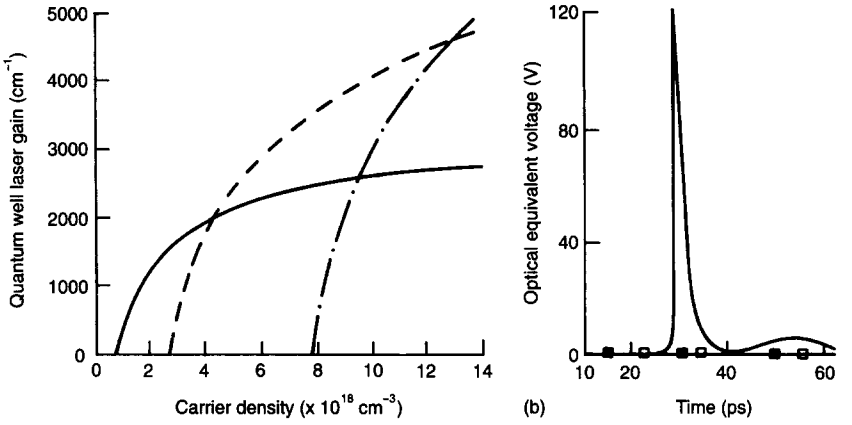

Figure 7 (a) Variation of gain with carrier density for various quantized levels. n: (——) 1, (– –) 2, (· – ·) 3. (b) Observation of gain-switched picosecond pulse due to the third quantized level transition. Cavity length, $L = 140\,\mu$m. FWHM = 2 ps. (□) QST1, (■) QST2.

Using Equation 8 for carrier density, $f_c - f_v$ can be expressed as:

$$f_c - f_v = 1 - \exp\{-(n/D1)\} - \exp\{-(n/D2)\} \tag{9}$$

where $D1$ and $D2$ are constants given by:

$$D1 = \frac{4\pi m_c^* KT}{h^2 L_z} \tag{10}$$

$$D2 = \frac{4\pi m_v^* KT}{h^2 L_z} \tag{11}$$

substituting Equation 9 into Equation 3, the gain for the $n = 1$ transition can be written as:

$$g_{m1} = K[1 - \exp\{-(n/D1)\} - \exp\{-(n/D2)\}] \tag{12}$$

As the density of the states in the second quantized level transition is double that of the $n = 1$ transition [14], the expression for optical gain for $n = 2$ can be written as:

$$g_{m2} = 2K[f_c(E_{f_c}, E_{c_2}) - f_v(E_{f_v}, E_{v_2})] \tag{13}$$

where E_{c_2} and E_{v_2} are the energy levels of the second conduction and valence sub-band, respectively; and f_c and f_v are Fermi distribution functions, that can be expressed as a function of carrier concentrations for the second quantized level transition in the following manner [15]:

$$N = D1\{\ln[1 + \exp(E_{f_c} - E_{c_1})/KT] + \ln[1 + \exp(E_{f_c} - E_{c_2})/KT]\} \tag{14}$$

where $D1$ is a constant as defined in Equation 10. E_{c_1} and E_{c_2} are confinement energies for $n = 1$ and $n = 2$ transitions, respectively. E_{f_c} is related to the density of electrons injected into the well. The expression for $f_c(E_{f_c}, E_{c_2})$ is given by:

$$f_c = \{1 + \exp[(E_{c_2} - E_{f_c})/KT]\}^{-1} \tag{15}$$

Using Equations 14 and 15, f_c can be written as:

$$f_c = \frac{[(x-1)^2 + 4xy]^{1/2} - (x+1)}{[(x-1)^2 + 4xy]^{1/2} + (x-1)} \tag{16}$$

where $x = \exp(E_{c_2} - E_{c_1}/KT)$ and $y = \exp(n/D1)$.

The expression for f_v can be obtained in a similar way:

$$f_v = \frac{2u}{(u-1)[(u-1)^2 + 4uv]^{1/2}} \tag{17}$$

where $u = \exp(E_{v_2} - E_{v_1}/KT)$ and $v = \exp(n/D2)$.

Substituting f_c and f_v from Equations 16 and 17 in Equation 13, the gain–carrier density relationship can be obtained for the $n = 2$ transition. Similarly, following the steps used for $n = 1$ and 2, the gain–carrier density relationship for the third quantized transition level ($n = 3$) can be evaluated.

Equations 1 and 2 for $i = 1$, 2 and 3 are used to construct the circuit model that includes the effect of QST3. Using the circuit model given in Fig. 1, the FWHM of the output pulse (observed at output node P3, Fig. 7b) has been reduced by about 70 per cent. Typical values used in the simulation are given in Table I.

3. Conclusions

In conclusion, circuit models that include the effects of the second and third quantized level transitions in quantum well lasers have been developed. Further, gain-switched picosecond pulses for 7 and 2 ps FWHM for the two quantized levels, respectively, were observed by simulating the models. The results indicate the applicability of the circuit modelling technique to the study of the gain-switching characteristics of multiple QW lasers.

References

1. H. LUI, M. FUKAZAWA, Y. KAWAL and T. KAMIYA, *IEEE J. Quantum Electron.* **25** (1989) 1417.
2. Y. ARAKAWA, T. SOGAWA, M. NISHIOKA, M. TANAKA and H. SAKAKI, *Appl. Phys. Lett.* **51** (1987) 1295.
3. R. NAGARAJAN, T. KAMIYA, A. KASUKAWA and H. OKAMOTO, *Appl. Phys. Lett.* **55** (1989) 1273.
4. P. P. VASIL'EV, *Opt. Quantum Electron.* **24** (1992) 801.
5. H. JUNG, E. SCHLOSSER and R. DEUFEL, *Appl. Phys. Lett.* **60** (1992) 401.
6. A. LARSSON and C. LINDSTRÖM, *Appl. Phys. Lett.* **54** (1989) 884.
7. R. S. TUCKER, *IEE Proc.* **128** (1981) 180.
8. R. S. TUCKER and D. J. POPE, *IEEE Trans. Microwave Theory Tech.* **31** (1983) 289.
9. J. E. A. WHITEAWAY, A. P. WRIGHT, B. GARRETT *et al.*, *Opt. Quantum Electron.* **26** (1994) S817.
10. N. K. DUTTA, *Electron. Lett.* **18** (1982) 451.
11. H. KOBAYASHI, H. IWAMURA, T. SAKU and K. OTSUKA, *Electron. Lett.* **19** (1983) 166.
12. D. MARCUSE, *IEEE J. Quantum Electron.* **19** (1983) 63.
13. B. SAINT-CRICQ, F. LOZES-DUPUY and G. VASSILIEFF, *IEEE J. Quantum Electron.* **22** (1986) 625.
14. A. YARIV, *Quantum Electronics*, 3rd edn (Wiley, Singapore, 1989).
15. M ASADA, A. KAMEYAMA and Y. SUEMATSU, *J. Quantum Electron.* **20** (1984) 745.